

# Combinatorial Fabrication of Fluorescent Patterns with Metal Ions Using Soft Lithography\*\*

By Lourdes Basabe-Desmonts, David N. Reinhoudt, and Mercedes Crego-Calama\*

Chemical pattern fabrication is an important issue in many fields ranging from microelectronics to biological microarray production, fabrication of sensor arrays, and nanotechnology.<sup>[1,2]</sup> Soft-lithography techniques, such as microcontact printing ( $\mu$ CP) and dip-pen nanolithography (DPN), are frequently used to pattern surfaces,<sup>[3,4]</sup> mainly by immobilizing a self-assembled monolayer (SAM) onto a bare substrate; the monolayer acts as an etch resist.<sup>[3]</sup> Conventional  $\mu$ CP is an efficient, low-cost method for patterning with feature sizes between 350 nm and a few millimeters.<sup>[3]</sup> The targets printed on SAMs<sup>[3]</sup> vary from (bio)molecules of different size, to catalysts,<sup>[5]</sup> polymers,<sup>[6]</sup> and dendrimers,<sup>[7]</sup> and, only recently, metal salts.<sup>[8,9]</sup>  $\mu$ CP can also be used to construct functionalized patterns on a surface through the covalent attachment of molecules to a reactive monolayer,<sup>[10–12]</sup> or through noncovalent synthesis using supramolecular interactions for the immobilization of molecules on functionalized surfaces.<sup>[7]</sup>

Many procedures for the direct fabrication and visualization of functional monolayer patterns often rely on specific binding between molecules. Specific interactions between antibodies and antigens are often used for the fabrication and visualization of patterned surfaces for biosensing applications.<sup>[13]</sup> Smart methods like affinity  $\mu$ CP have been used to produce reproducible protein arrays.<sup>[14]</sup> Metal–ligand and other supramolecular interactions have been used to build up 3D structures on a solid substrate.<sup>[15]</sup> Nevertheless, the diversity of patterned monolayer structures is often restricted by the elaborate design and limited number of substrate–ligand pairs with highly specific interactions. Even though soft-lithography techniques have been applied to combinatorial methods, the scope of these studies has been limited to the immobilization of arrays of proteins<sup>[16]</sup> or nanocrystals<sup>[17]</sup> on surfaces, and to the optimization of the patterning of (molecular) organic semiconductors by organic vapor jet printing.<sup>[18]</sup> The properties of polymers anchored to surfaces have also been studied by combinatorial methods.<sup>[19]</sup> In all these cases, applications are restricted to a unique, printable substrate, and cannot be systematically expanded to use different ligand–substrate combinations. In contrast to these specificity based patterning

methods, this paper describes a novel combinatorial approach for the generation of libraries of chemically patterned surfaces by  $\mu$ CP based on different combinations of substrate–adsorbate interactions.

A new sensing paradigm, based on the fabrication of SAMs on glass for cation sensing, recently developed by us,<sup>[12]</sup> is used here to prepare fluorescent substrates that are able to retain different metal-ion patterns. The metal-ion–ligand patterns are prepared by the deposition of metal salts onto these fluorescent materials by  $\mu$ CP. First, a library<sup>[20]</sup> of fluorescent SAMs ( $F_x, L_y$ ) ( $x, y = 1, 2, 3, \dots, n$ ) (Fig. 1a) are made by the sequential deposition of fluorophores,  $F_x$  ( $x = 1, 2, 3, \dots, n$ ), and ligand molecules,  $L_y$  ( $y = 1, 2, 3, \dots, n$ ), onto amino-terminated monolayers on glass. Each component of this library is a fluorescent glass substrate with different complexing abilities. Modulation of the fluorescence, that is, different degrees of fluorescence enhancement or quenching, is achieved by delivering different metal ions  $M_z$  ( $z = 1, 2, 3, \dots, n$ ) onto the monolayer by  $\mu$ CP. This fluorescence modulation is produced in the contact areas between the stamp and the fluorescent SAM. In this way, a library of patterns is obtained, where each pattern  $P(F_x, L_y, M_z)$  is the result of a combination of three building blocks, that is, a fluorophore, a ligand molecule, and a metal ion.

Besides the simplicity of the pattern generation, our approach offers the advantage of an easy high-throughput analysis, since the generated patterns can be visualized using fluorescence microscopy, without additional labeling steps. Thus, more demanding and sophisticated scanning probe microscopy techniques, such as atomic force microscopy (AFM), usually used for the characterization of patterned monolayer surfaces with high spatial resolution,<sup>[21]</sup> are avoided. Moreover, depending on the fluorescence technique, small or large areas of the patterned surface can be imaged with a resolution ranging from nanometers to millimeters.<sup>[22]</sup> Furthermore, these patterns can also be easily erased upon exposure to an appropriate environment, for example, a solvent or a competitive analyte.

As a proof of principle, the printing of several metal ions,  $\text{Cu}^{2+}$ ,  $\text{Co}^{2+}$ ,  $\text{Ca}^{2+}$ , and  $\text{Pb}^{2+}$ , onto differently functionalized fluorescent SAMs, TM1, TM2, and L0 (Fig. 1), has been studied using a poly(dimethylsiloxane) (PDMS) stamp. For the fabrication of the fluorescent glass substrates, an amino-terminated SAM *N*-[3-(trimethoxysilyl)propyl]ethylenediamine (TPEDA) (Fig. 1b) was functionalized with different pairs of fluorophore–ligand molecules. This allowed for parallel generation of multiple fluorescent monolayers with different complexing and sensing properties for a variety of metal ions.<sup>[11]</sup> For example, reaction of the TPEDA monolayer with

[\*] Prof. M. Crego-Calama, Dr. L. Basabe-Desmonts, Prof. D. N. Reinhoudt  
Department of Supramolecular Chemistry and Technology  
MESA<sup>+</sup> Institute for Nanotechnology, University of Twente  
P.O. Box 217, 7500 AE Enschede (The Netherlands)  
E-mail: m.cregocalama@utwente.nl

[\*\*] Supporting Information is available online from Wiley InterScience or from the author.

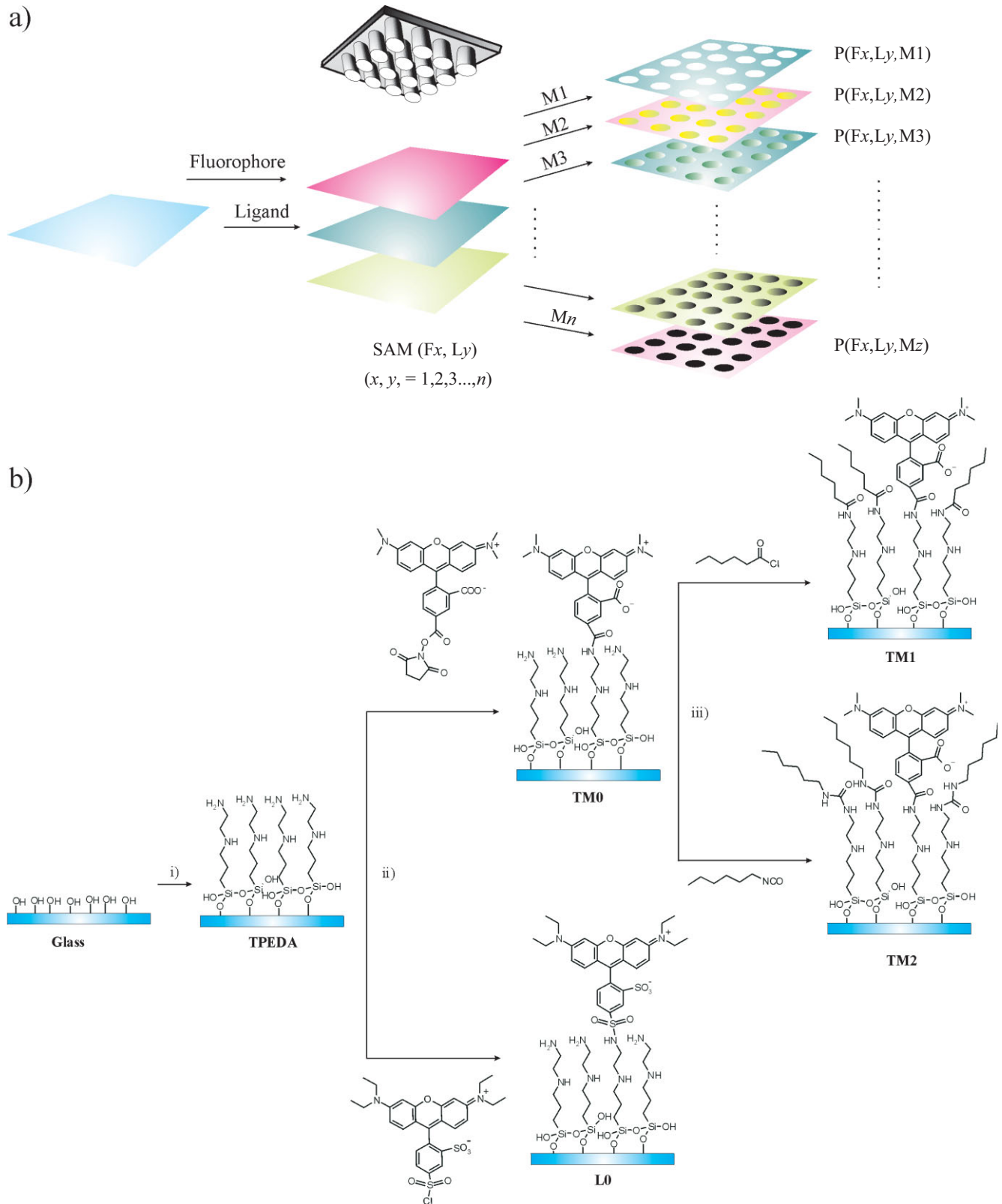


**Figure 1.** a) Representation of a generic fluorescent SAM library. SAM (F<sub>x</sub>,L<sub>y</sub>) (*x,y*=1,2,3,...,*n*) created by the combination of fluorophores (F1, F2,..., F<sub>n</sub>) and ligand molecules (L1, L2,..., L<sub>n</sub>). The dot arrays are microcontact printed using different metal-ion inks (M1, M2,..., M<sub>n</sub>) to create a library of patterned glass surfaces P(F<sub>x</sub>,L<sub>y</sub>,M<sub>z</sub>). b) Synthetic scheme of four different fluorescent SAMs. i) TPEDA, toluene, room temperature, 3.5 h, ii) 5(6)-TAMRA and Lissamine, to yield TM0 and L0 SAMs, respectively (acetonitrile, room temperature, 4 h), and iii) hexanoyl chloride and hexyl isocyanate, to afford the layers TM1 and TM2, respectively (chloroform, room temperature, 16 h).

the fluorophores 5(6)-TAMRA (5(6)-carboxytetramethylrhodamine, succinimidyl ester) and Lissamine (rhodamine B, sulfonil chloride) yielded the fluorescent SAMs, TM0 and L0, respectively (Fig. 1b). The remaining free amino groups were subsequently functionalized with smaller ligand molecules. Reaction of the fluorescent layer, TM0, with hexanoyl chloride or hexyl isocyanate resulted in the formation of the layers TM1 and TM2, respectively. After fabrication of the fluorescent monolayers, a PDMS stamp was used to deliver the metal ions by  $\mu$ CP onto the specific areas where the stamp was brought into contact with the functionalized substrate.

Four different metal ions,  $\text{Cu}^{2+}$ ,  $\text{Co}^{2+}$ ,  $\text{Ca}^{2+}$ , and  $\text{Pb}^{2+}$ , were transferred by  $\mu$ CP onto the TM1 SAM. The printing experiments were performed using freshly prepared PDMS stamps with 10  $\mu\text{m}$  dot features separated by a distance of 5  $\mu\text{m}$ ,

inked with different metal-ion solutions.<sup>[23,24]</sup> After the  $\mu$ CP process, the layers were imaged using fluorescence microscopy. The images showed that the fluorescence-emission intensity of the glass substrate areas where the metal ion was printed had changed. Comparing the patterns produced by  $\mu$ CP of the different metal ions (Fig. 2a) shows that  $\text{Pb}^{2+}$  and  $\text{Ca}^{2+}$  induce an enhancement of the fluorescence intensity of the native monolayer, creating a pattern with brighter dots, while  $\text{Co}^{2+}$  and  $\text{Cu}^{2+}$  metal ions quench the initial fluorescence intensity, resulting in a pattern with darker dots.<sup>[25]</sup> Remarkably,  $\text{Ca}^{2+}$  ions produced a higher fluorescence-intensity enhancement than  $\text{Pb}^{2+}$  ions. Furthermore, the quenching effect produced by  $\text{Cu}^{2+}$ -ion deposition was slightly higher than the quenching by the  $\text{Co}^{2+}$  ions. Additionally, the fluorescent patterns could be easily erased by washing away the printed

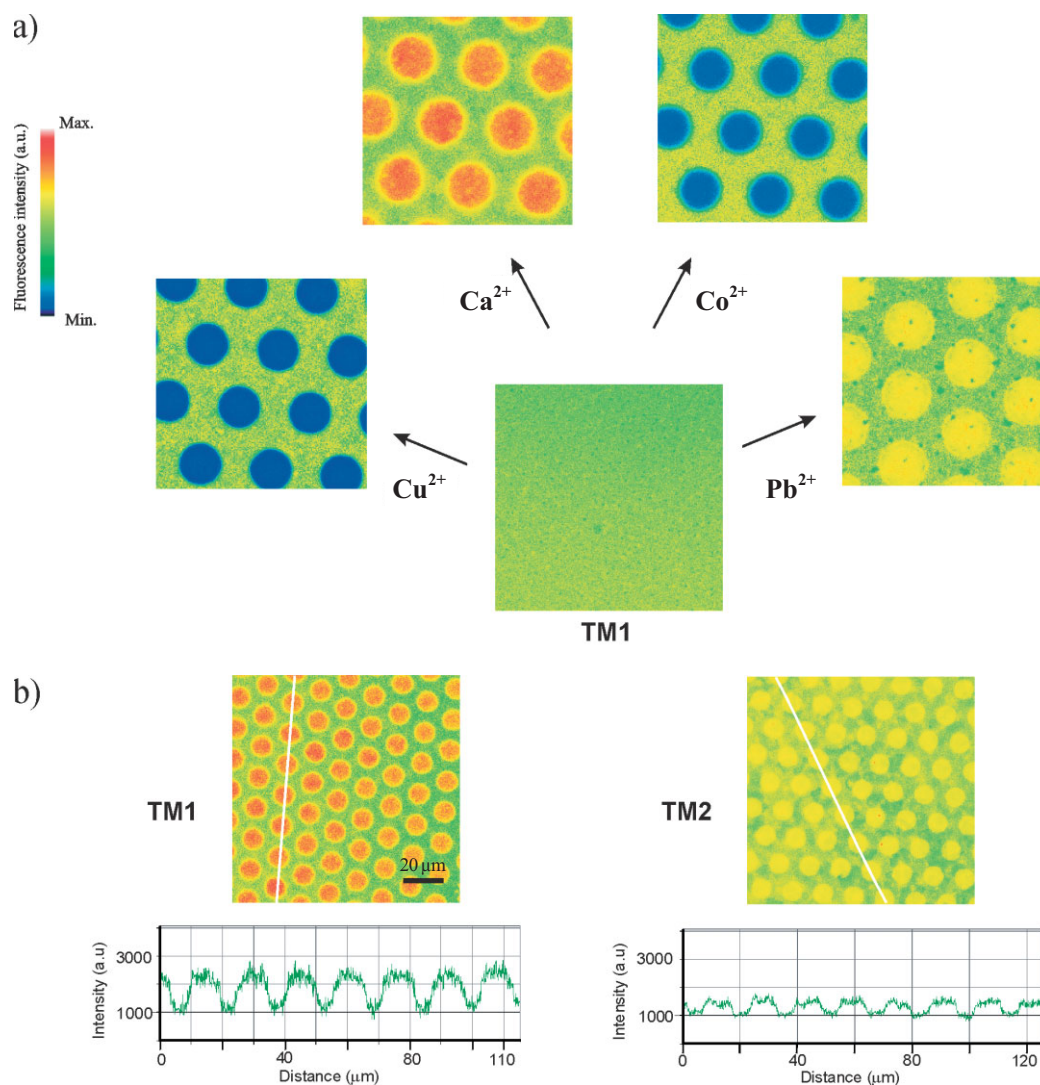


**Figure 2.** a) Fluorescence microscopy images of a TM1 SAM onto which  $\text{Cu}^{2+}$ ,  $\text{Ca}^{2+}$ ,  $\text{Co}^{2+}$ , and  $\text{Pb}^{2+}$  ions ( $10^{-3}$  M, acetonitrile) were printed using a PDMS stamp with 10  $\mu\text{m}$  diameter dot features, separated by a distance of 5  $\mu\text{m}$ . The image without dots corresponds to the initial fluorescence image of the TM1 SAM before printing of the metal ions. The color bar on the left represents the fluorescence-emission-intensity scale of the images. b) Fluorescence microscopy images (and the fluorescence-intensity profile of its cross sections defined by the white line) of TM1 and TM2 SAMs onto which  $\text{Ca}^{2+}$  ( $10^{-3}$  M, acetonitrile) has been microcontact printed with a 10  $\mu\text{m}$ -dot-array-featured PDMS stamp. For comparison, the images were normalized, the black horizontal line shows the initial fluorescence of the layers before printing of the analyte.

metal salt with HCl (0.1 M, aqueous solution), resulting in the recovery of the initial fluorescence.

To highlight the possibilities of this combinatorial approach,<sup>[26]</sup> similar printing experiments were performed with a different fluorescent glass substrate, TM2, which, compared to TM1, contains the same fluorophore but a different ligand molecule, that is, hexylurea instead of hexylamide. Fluorescence images of TM1 and TM2 SAMs were taken after  $\mu$ CP of  $\text{Ca}^{2+}$ ,  $\text{Cu}^{2+}$ , and  $\text{Pb}^{2+}$  ions (perchlorate salts, acetonitrile) using a stamp with a 10  $\mu\text{m}$  dot array. Comparing the patterns created on both substrates upon printing, for example, of the  $\text{Ca}^{2+}$  ions ( $10^{-3}$  M, acetonitrile), shows that the largest fluorescence enhancement is obtained for the TM1 layer (Fig. 2b). Similarly, the quenching produced by the  $\text{Cu}^{2+}$  ink ( $10^{-3}$  M, acetonitrile) was much more intense for the TM1 SAM (100 %) than for the TM2 SAM (50 %). However, when  $\text{Pb}^{2+}$  ink ( $10^{-2}$  M, acetonitrile) was used, both substrates displayed a pattern with almost the same fluorescence intensity (images not shown, see Supporting Information). These differences in the fluorescence intensity are remarkable since the TM1 and TM2 substrates differ only in the presence of amido (TM1) or ureido (TM2) groups. The mechanism for the perturbation of the fluorescence properties of the monolayers by the metal ions is not well understood yet. The type of ligating functionality and its distribution across the layer, together with possible steric constraints or additional surface interactions, such as monolayer packing, van der Waals forces, and cation– $\pi$ , and  $\pi$ – $\pi$  interactions, may determine the properties of the layers, and therefore the response towards different metal ions. Cation-controlled photoinduced processes, such as photoinduced electron transfer and charge transfer, may be responsible for the fluorescence perturbation.<sup>[27]</sup> On the other hand, the fluorescent monolayers that are well populated with other binding groups may very well act as a chemical ensemble, wherein a ligating-group/fluorophore assembly is selectively dissociated by the addition of an appropriate competitive analyte. This analyte may be able to interact efficiently with the ligating group, resulting in a detectable response from the fluorophore. Therefore, if the ligating groups are already quenching the fluorescence, it is possible that “unquenching” can be induced by the addition of an analyte, resulting in an increased fluorescence. If the binding groups are not quenching, the fluorescence is already at a maximum and no increase is expected. Therefore, modulation of the initial fluorescence may differ depending on the layer composition and the applied analyte.

Blank experiments have been performed to rule out any influence of the printing process on the fluorescence of the surface. Printing experiments using neat acetonitrile solution (without metal ions) yielded nonpatterned surfaces. Additionally, a set of experiments where the metal concentration in the ink solution was changed revealed that the intensity of the fluorescent patterns was dependent on the metal-ion concentration (see Supporting Information).

The same printing procedure has been applied to a different substrate–metal-ion combination, that is, an L0 SAM as the substrate, which comprises a TPEDA SAM functionalized

with the Lissamine fluorophore (Fig. 1b), and  $\text{Cu}^{2+}$  ( $10^{-3}$  M  $\text{Cu}(\text{ClO}_4)_2$  in water)<sup>[28]</sup> as the metal ion. A stamp with circuit features was used for printing. Figure 3 shows sections of the fluorescence image of a glass substrate coated with an L0 SAM after successful transfer of a circuit-shaped pattern of  $\text{Cu}^{2+}$  ions onto the monolayer. The ionic pattern created with features ranging from 2–100  $\mu\text{m}$  was well defined and could be directly visualized using fluorescence microscopy, owing to the fluorescence quenching of the layer where the deposition of  $\text{Cu}^{2+}$  ions took place.

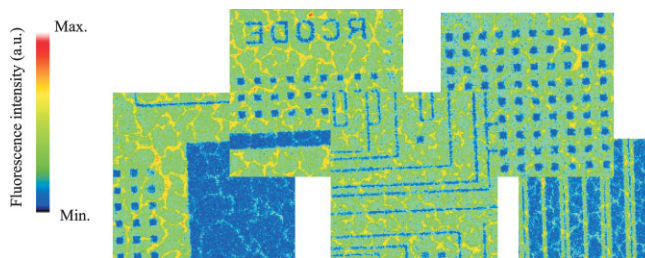


**Figure 3.** Different sections of a fluorescence confocal microscopy image of a glass slide coated with an L0 SAM in which  $\text{Cu}^{2+}$  ( $10^{-3}$  M  $\text{Cu}(\text{ClO}_4)_2$  in water [28]) was printed with a PDMS stamp with circuit features ranging from 2 to 100  $\mu\text{m}$ . The blue features correspond to areas where the fluorescence is quenched upon the deposition of  $\text{Cu}^{2+}$  ions.

This experiment showed that the transfer and direct visualization of any pattern on an elastomeric stamp is possible by simply inking the stamp with metal ions and printing onto a fluorescent surface. Additionally, fluorescence microscopy allows the visualization of large patterned monolayer areas more easily than other surface analytical techniques, such as AFM, which is limited to smaller-sized images<sup>[22]</sup> (see Supporting Information).

In conclusion, a new methodology for pattern generation and visualization has been presented. The process is based on a combinatorial approach,<sup>[26]</sup> where a proper combination of fluorescent SAMs and metal ions and the use of  $\mu$ CP results in the fabrication and screening of metal-ion patterns. The strength of this new combinatorial lithography is its potential implementation as a high-throughput process for the generation of metal-ion and fluorescent patterns. This results from the use of simple and easily accessible technologies, such as monolayer chemistry to produce fluorescent complexing glass substrates,  $\mu$ CP to transfer metal ions to the monolayers, and fluorescence microscopy to analyze the created patterns. We are currently attempting to scale down this approach to the nanoscale level by using DPN to write and erase fluorescent and ionic patterns on surfaces. Experiments to fabricate high-resolution and high-contrast patterns of metals by electroless deposition<sup>[29]</sup> are being carried out in our laboratories.

## Experimental

**Synthesis of the TPEDA SAM:** Formation of the TPEDA SAM was achieved in a glovebox under an atmosphere of dry nitrogen. The freshly cleaned substrate (15 min in piranha solution (concentrated

H<sub>2</sub>SO<sub>4</sub>/33% aqueous H<sub>2</sub>O<sub>2</sub> in a 3:1 ratio) Caution: piranha is a very strong oxidant and reacts violently with many organic materials) was immersed in TPEDA (5 mm) in dry toluene (freshly distilled over sodium) for 3.5 h. When the substrate was taken from the solution, it was rinsed twice with toluene (under a nitrogen atmosphere) to remove excess silane and avoid polymerization. The substrates were then removed from the glovebox and rinsed with EtOH and CH<sub>2</sub>Cl<sub>2</sub> to remove physisorbed material. The following protocol was repeated twice: stirring of the slide in a beaker filled with EtOH, then rinsing with a stream of EtOH, followed by stirring in CH<sub>2</sub>Cl<sub>2</sub>, then rinsing with a stream of CH<sub>2</sub>Cl<sub>2</sub>. The slides were then dried under an air stream.

**Synthesis of the TM0 and L0 SAMs:** The attachment of the fluorophores to the TPEDA SAM was achieved by immersing the slide for 4 h in a 0.23 mM acetonitrile solution of the fluorophores 5(6)-TAM-RA, SE (\*mixed isomers) and fluorophore Lissamine (rhodamine B, sulfonyl chloride) to yield TM0 and L0. Et<sub>3</sub>N (100 μL) was added to the Lissamine solutions. All reactions were carried out in a glovebox under an atmosphere of dry nitrogen. After the substrates were taken out of the solution they were rinsed with CH<sub>3</sub>CN, EtOH, and CH<sub>2</sub>Cl<sub>2</sub> to remove physisorbed material. The slides were then dried under an air stream.

**Synthesis of the TM1 and TM2 SAMs:** The TM0-functionalized slides were immersed in a CH<sub>3</sub>CN solution of hexanoyl chloride (50 mM) and hexyl isocyanate (12 mM) to afford TM1 and TM2, respectively. Et<sub>3</sub>N (100 μL) was added to the hexanoyl chloride solution. All reactions were carried out under an atmosphere of dry nitrogen for 16 h. When the substrates were taken out of the solution they were rinsed sequentially with CH<sub>3</sub>CN, EtOH, and CH<sub>2</sub>Cl<sub>2</sub> to remove physisorbed material. The slides were then dried under an air stream.

**Characterization of the Monolayers:** All the layers were characterized by contact-angle goniometry, ellipsometry, and fluorescence spectroscopy. Additionally and to assure the introduction of the binding groups, X-ray photoelectron spectroscopy (XPS) measurements were performed. Values of the individual advancing/receding contact angles ( $\theta_a/\theta_r$ ), as well as the hysteresis values ( $\theta_a - \theta_r$ ) reflect a variation in the surface hydrophobicity, and therefore variation in the surface functionalization ( $\theta_a/\theta_r$  [°]) TM0 = 69/32, TM1 = 89/75, TM2 = 55/35, L0 = 63/35). Ellipsometry measurements were performed on silicon wafers. The experimental monolayer thicknesses are in good agreement with the thickness modeled with CPK models (software WebLab Viewer v2.01) The experimental thicknesses obtained were TM0 = 1.33 ± 0.04 nm, TM1 = 1.28 ± 0.30 nm, TM2 = 1.13 ± 0.28 nm, L0 = 1.32 ± 0.15 nm. Fluorescence spectroscopy confirmed the introduction of the fluorophores, maximum emission peaks appeared at  $\lambda = 588$  nm for L0 and  $\lambda = 585$  nm for TM0. To investigate the surface coverage of the samples after functionalization with the binding molecules, we marked the binding molecule with an XPS-sensitive label. The XPS spectrum confirmed successful functionalization of the fluorescent monolayer with binding molecules [10].

Received: August 2, 2005  
Final version: January 26, 2006

- [1] Y. N. Xia, J. A. Rogers, K. E. Paul, G. M. Whitesides, *Chem. Rev.* **1999**, *99*, 1823.
- [2] M. T. Bohr, *IEEE Trans. Nanotechnol.* **2002**, *1*, 56.
- [3] M. Geissler, Y. N. Xia, *Adv. Mater.* **2004**, *16*, 1249.
- [4] D. S. Ginger, H. Zhang, C. A. Mirkin, *Angew. Chem. Int. Ed.* **2004**, *43*, 30.
- [5] E. Delamarche, C. Donzel, F. S. Kamounah, H. Wolf, M. Geissler, R. Stutz, P. Schmidt-Winkel, B. Michel, H. J. Mathieu, K. Schaumburg, *Langmuir* **2003**, *19*, 8749.
- [6] H. P. Zheng, M. F. Rubner, P. T. Hammond, *Langmuir* **2002**, *18*, 4505.
- [7] T. Auletta, B. Dordi, A. Mulder, A. Sartori, S. Onclin, C. M. Bruinink, M. Peter, C. A. Nijhuis, H. Beijleveld, H. Schonherr, G. J. Vancso, A. Casnati, R. Ungaro, B. J. Ravoo, J. Huskens, D. N. Reinhoudt, *Angew. Chem. Int. Ed.* **2004**, *43*, 369.
- [8] K. L. Yang, K. Cadwell, N. L. Abbott, *Adv. Mater.* **2003**, *15*, 1819.
- [9] L. A. Porter, H. C. Choi, J. M. Schmeltzer, A. E. Ribbe, L. C. C. Elliott, J. M. Buriak, *Nano Lett.* **2002**, *2*, 1369.
- [10] L. Basabe-Desmots, J. Beld, R. S. Zimmerman, J. Hernando, P. Mela, M. F. G. Parajo, N. F. Van Hulst, A. Van Den Berg, D. N. Reinhoudt, M. Crego-Calama, *J. Am. Chem. Soc.* **2004**, *126*, 7293.
- [11] R. S. Zimmerman, L. Basabe-Desmots, F. van der Baan, D. N. Reinhoudt, M. Crego-Calama, *J. Mater. Chem.* **2005**, *15*, 2772.
- [12] M. Crego-Calama, D. N. Reinhoudt, *Adv. Mater.* **2001**, *13*, 1171.
- [13] A. Bernard, J. P. Renault, B. Michel, H. R. Bosshard, E. Delamarche, *Adv. Mater.* **2000**, *12*, 1067.
- [14] J. P. Renault, A. Bernard, D. Juncker, B. Michel, H. R. Bosshard, E. Delamarche, *Angew. Chem. Int. Ed.* **2002**, *41*, 2320.
- [15] V. Mahalingam, S. Onclin, M. Peter, B. J. Ravoo, J. Huskens, D. N. Reinhoudt, *Langmuir* **2004**, *20*, 11756.
- [16] D. Stoll, M. F. Templin, M. Schrenk, P. C. Traub, C. F. Vohringer, T. O. Joos, *Frontiers Biosci.* **2002**, *7*, C13.
- [17] T. Vossmeier, S. Jia, E. Delonno, M. R. Diehl, S. H. Kim, X. Peng, A. P. Alivisatos, J. R. Heath, *J. Appl. Phys.* **1998**, *84*, 3664.
- [18] M. Shtein, P. Peumans, J. B. Benziger, S. R. Forrest, *J. Appl. Phys.* **2004**, *96*, 4500.
- [19] T. Wu, M. Tomlinson, K. Efimenko, J. Genzer, *J. Mater. Sci.* **2003**, *38*, 4471.
- [20] The term library used here refers to a set of glass slides with each slide functionalized with a different fluorescent monolayer resulting from the combination of a unique fluorophore and a unique ligand molecule.
- [21] M. E. Greene, C. R. Kinser, D. E. Kramer, L. S. C. Pingree, M. C. Hersam, *Microsc. Res. Techn.* **2004**, *64*, 415.
- [22] Even though STM and AFM have a much higher spatial resolution than fluorescence techniques (2 nm as compared to half of the wavelength of the excitation light, around 270 nm in this case), standard AFM and STM techniques have a limited ability to produce images of areas below 250 μm × 250 μm, while fluorescence techniques can be used to image much larger areas, from nanometer to centimeter size. XPS mapping is the only instrumental method that has been shown to be useful for imaging millimeter-sized areas but it has a spatial resolution of 10 μm, which limits the technique to the visualization of patterns with large features. Additionally, XPS is a much less accessible technique.
- [23] Before inking, the stamps were oxidized by exposing them to UV/ozone for 60 min. This process enhanced the hydrophilicity of the stamp and homogeneous spreading of the ink [26]. After ozone treatment the stamps were directly introduced into 10<sup>-3</sup> M acetonitrile solutions of Pb<sup>2+</sup>, Co<sup>2+</sup>, Cu<sup>2+</sup>, and Ca<sup>2+</sup>, as perchlorate salts, for 15 min. Then, the stamps were dried in a nitrogen stream and brought into contact with the sensitive fluorescent substrate for 1 min [10].
- [24] A. Olah, H. Hillborg, G. J. Vancso, *Appl. Surf. Sci.* **2005**, *239*, 410.
- [25] The halos that surround the spots in some of the patterns correspond to higher (in the case of Ca<sup>2+</sup> and Pb<sup>2+</sup>) or lower (in the case of Co<sup>2+</sup>) concentrations of metal ions deposited on the surface due to lateral diffusion of the ink on the stamp surface, either towards the edges or the center of the spot.
- [26] In this work we use the term combinatorial approach to refer to the parallel fabrication of a library of patterns by the combination of three building blocks: a fluorophore, a ligand molecule, and a metal ion. Inks comprising metal-ion mixtures can also be used; this work is currently in progress.
- [27] B. Valeur, I. Leray, *Coord. Chem. Rev.* **2000**, *205*, 3.
- [28] The printing experiments in this article have been performed using metal-ion solutions in acetonitrile as ink, but additional experiments not shown here have revealed that aqueous inks spread less on the surface and better definition of the pattern can be obtained.
- [29] D. I. Ma, L. Shirey, D. McCarthy, A. Thompson, S. B. Qadri, W. J. Dressick, M. S. Chen, J. M. Calvert, R. Kapur, S. L. Brandow, *Chem. Mater.* **2002**, *14*, 4586.